ISSN: 2350-0328

International Journal of Advanced Research in Science, Engineering and Technology

Vol. 3, Issue 9 , September 2016

Pulsatile Flow of a Jeffrey Fluid Between Permeable Beds

P. Dhanalakshmi, S. Sreenadh, K. Sushma

Department of Mathematics, Sri Venkateswara University, Tirupati, A.P.

ABSTRACT: Pulsatile flow of a Jeffrey fluid between permeable beds is investigated. The flow between the permeable beds is assumed to be governed by Jeffrey model and that in the permeable beds by Darcy's law. The governing equations are solved analytically and the expressions for velocity and mass flux are obtained. The effects of the material parameters on the velocity and mass flux are studied numerically and the results are presented through graphs. It is found that the increasing Jeffrey parameter enhances the fluid velocity and mass flux in the channel.

I. INTRODUCTION

Pulsatile flow is a periodic flow that oscillates around a mean value not equal to zero, that is it is a steady flow on which is superposed an oscillatory flow. It has important biological applications in relation to hemodynamics and industrial applications in relation to heat exchange efficiency of IC engines. Literature survey reveals that most of the available research works deal with pulsatile flow of Newtonian fluids in the channels with or without permeable walls. But works on Non-Newtonian fluid flow concerning porous media is very limited. The coupled phenomenon of pulsating fluid flow and porous media is a problem of prime importance in geomechanics and biomechanics. One such problem is the study of hemodynamic effect of the endothelial glycocalyx.

In view of these applications,the study of pulsatile Non-Newtonian fluid flow is necessitated. Wang [1] studied the pulsatile flow of a viscous fluid in a porous channel. Vajravelu et al. [2] investigated the pulsatile flow of a Newtonian fluid between permeable beds.

In recent years, the study of non-Newtonian fluid flows are analysed because of its important applications in industry and physiology,for e.g. enhanced oil recovery and chemical process. Sankar et al. [3] studied the pulsatile flow of blood through catheterized artery by modeling blood as Herschel-Bulkley fluid and the catheter and artery as rigid coaxial circular cylinders. Perturbation method is used to solve the resulting quasi-steady nonlinear coupled implicit system of differential equations. The effects of catheterization and non- Newtonian nature of blood are discussed. Prashanta Kumar Mandal et al. [4]examined the laminar two dimensional pulsatile flow of blood under the influence of externally imposed periodic body acceleration through artery with stenosis. A mathematical model is developed bytreating blood as a non- Newtonian fluid characterized by the generalized Power law model incorporating both the shear thinning and shear thickening characteristics of the streaming blood. Krishnakumari et al. [5] recently investigated peristaltic pumping of a Jeffrey fluid in a porous tube under long wave length and low Reynolds number assumptions. Krishnakumari et al. [6] also studied the peristaltic transport of a Jeffrey fluid under the effect of magnetic field in an inclined channel. Akbar et al. [7]applied Jeffery fluid model for blood flow through a tapered artery with stenosis by assuming blood as Jeffrey fluid. Perturbation method is used to solve the governing equations. Srinivas et al. [8] investigated the peristaltic transport of a Jeffrey fluid under the effect of slip in an inclined asymmetric channel. The fluid is assumed to be incompressible and electrically conducting. The analytic solution has been derived for the stream function. The effect of slip and non-Newtonian parameter on the axial velocity and shear stress are discussed.
The study of pulsatile flow in a porous channel is important in the dialysis of blood in artificial kidneys and in extracting oil/water from the underground reservoirs. Furtherthe behaviorof blood flow in the circulatory system where the nutrients are supplied to tissues of various organs and waste products are removed.Vajravelu et al. [9] made a detailed study on the pulsatile flow between permeable beds. Sudhakara et al.[10] investigated the pulsatile flow of a hydromagneticjeffrey fluid between permeable beds. Hemadri Reddy et al. [11] investigated the effect of thickness of the porous material on the peristaltic pumping when the tube wall is provided with non-erodible porous lining. Vasudev et al. [12] discussed the interaction of heat transfer with peristaltic pumping of a Williamson fluid through a porous

ISSN: 2350-0328

International Journal of Advanced Research in Science, Engineering and Technology

Vol. 3, Issue 9 , September 2016

medium in a planar channel, under the assumptions of low Reynolds number and long wave length. Kim et al. [13] discussed the effects of membrane length and hydraulic resistance on the steady-state laminar flow of a fluid with injection in a cylindrical porous tube using the perturbation approach of the Navier-Stokes and continuity equations. Srinivas et al. [14] studied the effects of heat and mass transfer on peristaltic transport in a porous space with compliant walls. Vajravelu et al. [15] studied the interaction of peristalsis with heat transfer for the flow of a viscous fluid in a vertical porous annular region between two concentric tubes. Using the perturbation method, the solutions are obtained for the velocity and the temperature fields. Lalithajyothi et al. [16] studied the pulsatile flow of a jeffrey fluid in a circular tube having internal porous lining.Vajravelu et al. [17] investigated the unsteady flow of two immiscible conducting fluids between two permeable beds. Motivated by the above studies, pulsatile flow of a Jeffrey fluid between permeable beds is investigated. The fluid is driven by an unsteadypressure gradient and the effects of various physical parameters on the flow quantities are discussed through graphs and tables.

II. MATHEMATICAL FORMULATION OF THE PROBLEM

We consider the pulsatile flow of a Jeffrey fluid flow between permeable beds (see fig.1). The permeabilities of lower and upper beds are k_1 and k_2 respectively. The flow in upper and lower permeable beds is assumed to be governed by Darcy's law.

Let the x-axis (the flow direction) be taken midway between the beds and the y-axis be taken perpendicular to the beds. The following assumptions are made in the analysis of the problem:

(a) The permeable beds are homogeneous

(b) The flow is laminar and fully developed

(c) The fluid is driven by an unsteady

pressure gradient,

$$\frac{\partial p}{\partial x} = p_x e^{\text{int}} \qquad (1)$$

where p_x be the pressure and n is the frequency.

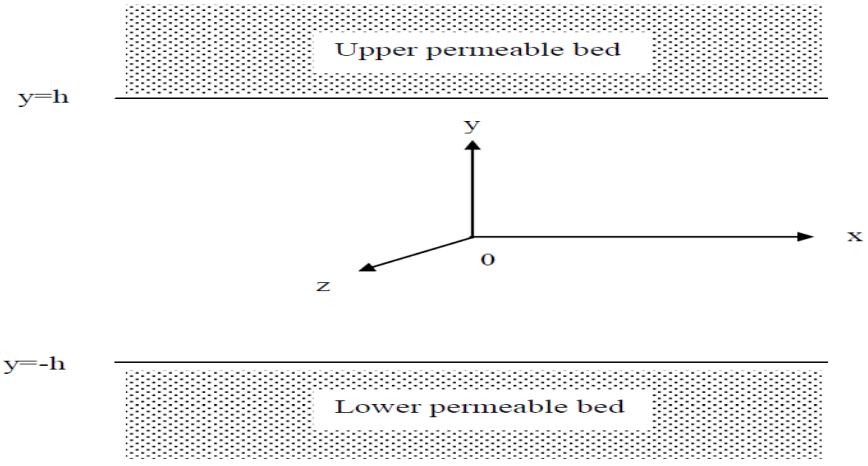

Fig.1. Physical model

In the absence of body forces and body couples, the governing equations of the problem are given by

$$\frac{\partial u}{\partial t} = \frac{-1}{\rho}\frac{\partial p}{\partial x} + \frac{\upsilon}{1+\lambda_1}\frac{\partial^2 u}{\partial y^2} \qquad (2)$$

$$\frac{1}{\varepsilon}\frac{\partial Q_i}{\partial t} = \frac{-1}{\rho}\frac{\partial p}{\partial x} - \frac{\upsilon}{(1+\lambda_1)k}Q_i \qquad (3)$$

ISSN: 2350-0328

International Journal of Advanced Research in Science, Engineering and Technology

Vol. 3, Issue 9 , September 2016

$$u = \mathrm{Re}\,al\,(w(y)e^{\mathrm{int}}),$$
$$Q_i = \mathrm{Re}\,al\,(S_{Q_i}(y)e^{\mathrm{int}}), \qquad (4)$$
$$u_{B_i} = \mathrm{Re}\,al\,(S_{B_i}e^{\mathrm{int}}), where\, i = 1,2$$

Where Real( ) denotes the real part of a complex number.

Herein the velocity component $u(y,t)$ is to satisfy the conditions

$$\left.\begin{aligned} u &= u_{B_1} \quad at \quad y = -h \\ u &= u_{B_2} \quad at \quad y = h \end{aligned}\right\} \qquad (5)$$

$$\left.\begin{aligned} \frac{\partial u}{\partial y} &= \frac{\alpha}{\sqrt{k_1}}(u_{B_1} - Q_1) \quad at \quad y = -h \\ \frac{\partial u}{\partial y} &= -\frac{\alpha}{\sqrt{k_2}}(u_{B_2} - Q_2)\ at \quad y = h \end{aligned}\right\} \qquad (6)$$

III. NON – DIMENSIONALISATION OF THE FLOW QUANTITIES

The following non-dimensional quantities are introduced to make the basic equations and the boundary conditions dimensionless

$$u^* = \frac{u}{U}, u_{B_{1,2}}{}^* = \frac{u_{B_{1,2}}}{U}, p^* = \frac{p}{\rho U^2}, t^* = \frac{tU}{h}, Q_{1,2}{}^* = \frac{Q_{1,2}}{U}, x^* = \frac{x}{h}, y^* = \frac{y}{h}, \mathrm{Re} = \frac{Uh}{\upsilon},$$

$$\sigma_1 = \frac{h}{\sqrt{k_1}}, \sigma_2 = \frac{h}{\sqrt{k_2}} \qquad (7)$$

$$\mathrm{Re}(1+\lambda_1)\left(\frac{\partial u^*}{\partial t^*} + \frac{\partial p^*}{\partial x^*}\right) = \frac{\partial^2 u^*}{\partial y^{*2}} \qquad (8)$$

$$\frac{\partial Q_i^*}{\partial t^*} + \frac{\varepsilon}{(1+\lambda_1)}\frac{\sigma^2}{\mathrm{Re}} Q_i^* = -\varepsilon\frac{\partial p^*}{\partial x^*} \qquad (9)$$

After neglecting asterisks (*), we get

$$\mathrm{Re}(1+\lambda_1)\left(\frac{\partial u}{\partial t} + \frac{\partial p}{\partial x}\right) = \frac{\partial^2 u}{\partial y^2} \qquad (10)$$

$$\frac{\partial Q_i}{\partial t} + \frac{\varepsilon}{(1+\lambda_1)}\frac{\sigma^2}{\mathrm{Re}} Q_i = -\varepsilon\frac{\partial p}{\partial x} \qquad (11)$$

$$\left.\begin{aligned} u &= u_{B_1} \quad at \quad y = -1 \\ u &= u_{B_2} \quad at \quad y = 1 \end{aligned}\right\} \qquad (12)$$

$$\left.\begin{aligned} \frac{\partial u}{\partial y} &= \frac{\alpha}{\sqrt{k_1}}(u_{B_1} - Q_1) \quad at \quad y = -1 \\ \frac{\partial u}{\partial y} &= -\frac{\alpha}{\sqrt{k_2}}(u_{B_2} - Q_2)\ at \quad y = 1 \end{aligned}\right\} \qquad (13)$$

ISSN: 2350-0328

International Journal of Advanced Research in Science, Engineering and Technology

Vol. 3, Issue 9 , September 2016

IV. SOLUTION OF THE PROBLEM

Solving Eqns. (10) and(11) subject to the conditions (12) and(13), we get the velocity field as

$$u=\left(u_{B_1}+u_{B_2}-\frac{-2ip_x}{n}\right)\left(\frac{\cosh\left((1+i)\sqrt{\frac{\mathrm{Re}(1+\lambda_1)n}{2}}\,y\right)}{2\cosh\left((1+i)\sqrt{\frac{\mathrm{Re}(1+\lambda_1)n}{2}}\right)}\right)+\left(u_{B_2}-u_{B_1}\right)$$

$$\left(\frac{\sinh\left((1+i)\sqrt{\frac{\mathrm{Re}(1+\lambda_1)n}{2}}\,y\right)}{2\sinh\left((1+i)\sqrt{\frac{\mathrm{Re}(1+\lambda_1)n}{2}}\right)}\right)+\frac{ip_x}{n} \qquad (14)$$

Where

$$Q_1=\frac{-\varepsilon P_x}{in+\frac{\varepsilon\sigma_1^{\,2}}{\mathrm{Re}(1+\lambda_1)}},\ Q_2=\frac{-\varepsilon P_x}{in+\frac{\varepsilon\sigma_2^{\,2}}{\mathrm{Re}(1+\lambda_1)}},\ A=\frac{-iP_x}{n\cosh\left[(1+i)\sqrt{\frac{\mathrm{Re}(1+\lambda_1)n}{2}}\right]},\ B=0$$

$$u_{B_1}=\left(\frac{1}{\alpha\sigma_1}\right)\left[\left((1+i)\sqrt{\frac{\mathrm{Re}(1+\lambda_1)n}{2}}\right)\left[-A\sinh\left((1+i)\sqrt{\frac{\mathrm{Re}(1+\lambda_1)n}{2}}\right)+B\cosh\left((1+i)\sqrt{\frac{\mathrm{Re}(1+\lambda_1)n}{2}}\right)\right]\right]+Q_1,$$

$$u_{B_2}=\left(\frac{-1}{\alpha\sigma_2}\right)\left[\left((1+i)\sqrt{\frac{\mathrm{Re}(1+\lambda_1)n}{2}}\right)\left[A\sinh\left((1+i)\sqrt{\frac{\mathrm{Re}(1+\lambda_1)n}{2}}\right)+B\cosh\left((1+i)\sqrt{\frac{\mathrm{Re}(1+\lambda_1)n}{2}}\right)\right]\right]+Q_2$$

V. DEDUCTIONS

Taking $k_1=k_2=k\,(\text{i.e.},\sigma_1=\sigma_2=\sigma)$ in Eqn. (14), we obtain the velocity field as follows

$$u=\left(u_{B_1}+u_{B_2}-\frac{-2ip_x}{n}\right)\left(\frac{\cosh\left((1+i)\sqrt{\frac{\mathrm{Re}(1+\lambda_1)n}{2}}\,y\right)}{2\cosh\left((1+i)\sqrt{\frac{\mathrm{Re}(1+\lambda_1)n}{2}}\right)}\right)+\left(u_{B_2}-u_{B_1}\right)\left(\frac{\sinh\left((1+i)\sqrt{\frac{\mathrm{Re}(1+\lambda_1)n}{2}}\,y\right)}{2\sinh\left((1+i)\sqrt{\frac{\mathrm{Re}(1+\lambda_1)n}{2}}\right)}\right)$$

$$+\frac{ip_x}{n} \qquad (15)$$

ISSN: 2350-0328

International Journal of Advanced Research in Science, Engineering and Technology

Vol. 3, Issue 9 , September 2016

Where

$$Q_1=\frac{-\varepsilon P_x}{in+\frac{\varepsilon\sigma^2}{\mathrm{Re}(1+\lambda_1)}},\ Q_2=\frac{-\varepsilon P_x}{in+\frac{\varepsilon\sigma^2}{\mathrm{Re}(1+\lambda_1)}},\ A=\frac{-iP_x}{n\cosh\left[(1+i)\sqrt{\frac{\mathrm{Re}(1+\lambda_1)n}{2}}\right]},\ B=0$$

$$u_{B_1}=\left(\frac{1}{\alpha\sigma}\right)\left[\left((1+i)\sqrt{\frac{\mathrm{Re}(1+\lambda_1)n}{2}}\right)\left[-A\sinh\left((1+i)\sqrt{\frac{\mathrm{Re}(1+\lambda_1)n}{2}}\right)+B\cosh\left((1+i)\sqrt{\frac{\mathrm{Re}(1+\lambda_1)n}{2}}\right)\right]\right]+Q_1,$$

$$u_{B_2}=\left(\frac{-1}{\alpha\sigma}\right)\left[\left((1+i)\sqrt{\frac{\mathrm{Re}(1+\lambda_1)n}{2}}\right)\left[A\sinh\left((1+i)\sqrt{\frac{\mathrm{Re}(1+\lambda_1)n}{2}}\right)+B\cosh\left((1+i)\sqrt{\frac{\mathrm{Re}(1+\lambda_1)n}{2}}\right)\right]\right]+Q_2$$

A. Mass flux

The mass flux in the channel bounded by beds is given by

$$Q=\int_{-h}^{h}udy \qquad (16)$$

B. Shear stress

The shear stresses at the lower and upper beds are given by

$$\tau=\frac{1}{(1+\lambda_1)\mathrm{Re}}\left(\frac{\partial u}{\partial y}\right)_{y=-1,1} \qquad (17)$$

VI. NUMERICAL RESULTS AND DISCUSSION

The expression for the fluid velocity u is evaluated numerically for different values of physical parameters such as the permeability parameter ε, porosity parameter σ, slip parameter α, Reynolds number Re, Jeffrey parameter λ_1 and nt and are shown in Figures 2 to 11 and Tables 1 to 6.

Figures 2 to 4 elucidate the variation of fluid velocity in the channel which is computed from eqn. (14), for different values of $\varepsilon, \sigma, \alpha$. It is noticed that the increase in the ε, σ, α, decreases with the velocity in the channel. Also it is found that the unsteady velocity component increases with increasing Re, λ_1 from figures 5 and 6. From figures 7 to 11, it is clear that the velocity decreases with the increasing values of nt.

The variation of mass flux is computed from eqn. (16) for different values of ε, σ, α, Re and λ_1 and it is displayed in Table 1. It is observed that the mass flux Q decreases with increasing ε, σ and α whereas it increases with the increasing of λ_1, Re as depicted in Table 1. This shows that the effect of permeable bed is to enhance the mass flux in the channel which is similar to the behaviour observed by Rajasekhara et al. [18].The non-Newtonian Jeffrey fluid pumps more fluid (and hence mass flux is more) when compared with Newtonian fluid.The variation of shear stress is computed from eqn. (17) for different values of ε, σ, α, Re and λ_1 parameters and are tabulated in Tables 2 to 6.For, $\pi/4 \le \omega t < \pi$, it is observed that the shear stress increases with the increase in the permeability parameter at the lower permeable bed whereas opposite behaviour is noticed at the upper permeability bed. Further, for the increase in the Reynolds number, porosity parameter, Jeffrey parameter and slip parameter, decreases the shear stress at lower permeable bed whereas opposite behaviour is observed at upper permeable bed.

ISSN: 2350-0328

International Journal of Advanced Research in Science, Engineering and Technology

Vol. 3, Issue 9 , September 2016

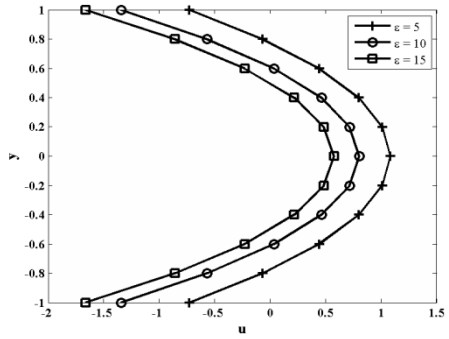

Fig.2. Velocity profile for α *=0.5, t=1,R=0.5,* σ_1 *=0.5,* σ_2 *=0.5,P=-1,* λ_1 *=0.1,* $n = 3\pi/4$

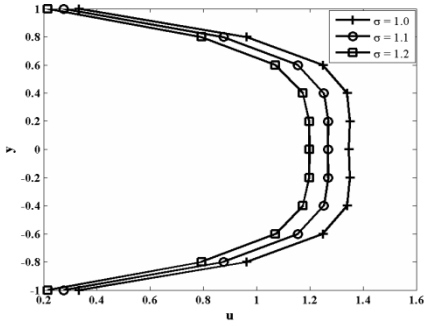

Fig.3. Velocity profile for α *=0.5, t=1,* ε *=2,P=-1,R=2,* λ_1 *=0.1,* $n = 3\pi/4$

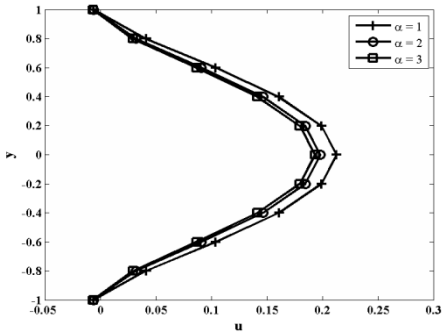

Fig.4. Velocity profile for σ *=15, t=1,* ε *=2, P=-1,R=2,* λ_1 *=0.1,* $n = 3\pi/4$

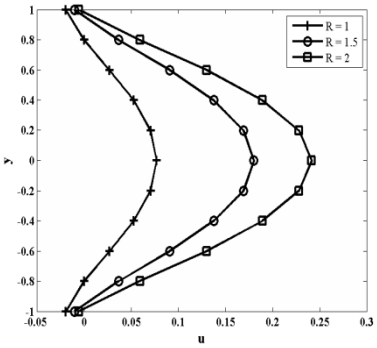

Fig.5.Velocity profile for σ *=15, t=1,* ε *=2,P=-1,* α *=0.5,* λ_1 *=0.1,* $n = 3\pi/4$

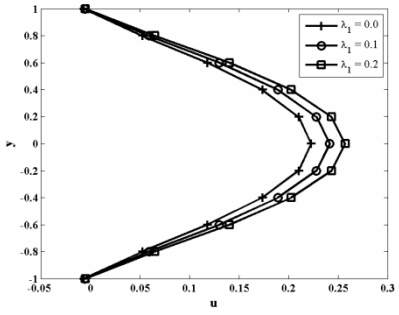

Fig.6.Velocity profile for σ *=15, t=1,* ε *=2,P=-1,* α *=0.5,* $n = 3\pi/4$ *,R=2*

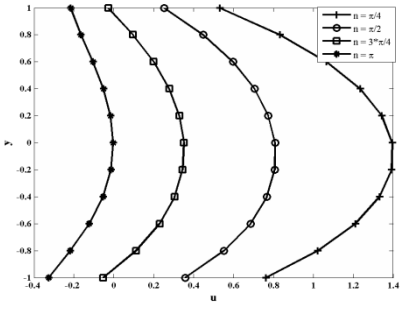

Fig.7.Velocity profile for σ_1 *=5,* σ_2 *=7, t=1, P=-1,* α *=0.5,R=2,* λ_1 *=0.1,* ε *=2*

ISSN: 2350-0328

International Journal of Advanced Research in Science, Engineering and Technology

Vol. 3, Issue 9 , September 2016

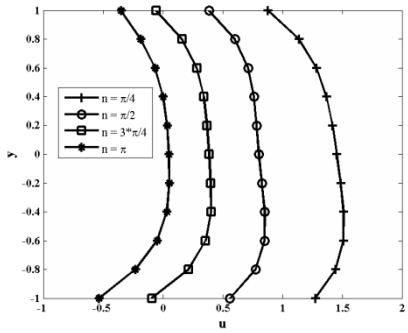

Fig.8. Velocity profile for $\sigma_1 = 5, \sigma_2 = 7$, *t=1, P=-1,* $\alpha = 0.5$, *R=4.5,* $\lambda_1 = 0.1, \varepsilon = 2$

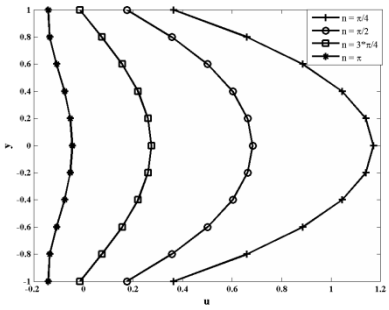

Fig.9. Velocity profile for $\sigma = 10$, *t=1,P=-1,* $\alpha = 0.5$, *R=2,* $\lambda_1 = 0.1, \varepsilon = 2$

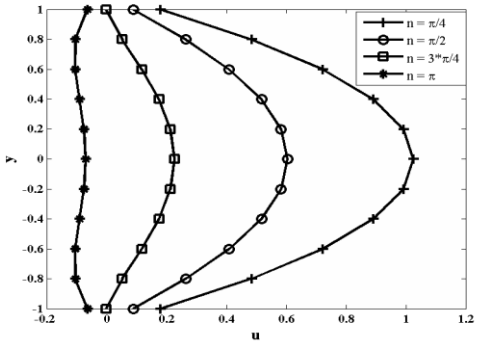

Fig.10.Velocity profile for $\sigma = 20$, *t=1, P=-1,* $\alpha = 0.5$, *R=2,* $\lambda_1 = 0.1, \varepsilon = 2$

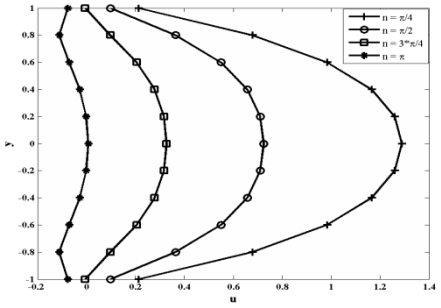

Fig. 11.Velocity profile for $\sigma_1 = 30$, $\sigma_2 = 30$, *t=1,P=-1,* $\alpha = 0.5$, *R=6,* $\lambda_1 = 0.1, \varepsilon = 2$

Table1: Effect of $\varepsilon, \sigma, \alpha, \lambda_1$ and Re on Mass flux Q or fixed values of $t = 1, n = \frac{3\pi}{4}$ and $P = -1$.

ε	σ	α	λ_1	Re	Q
2	1	0.5	0.1	1	1.6669
3	1	0.5	0.1	1	1.6354
4	1	0.5	0.1	1	1.5443
5	1	0.5	0.1	1	1.4503
6	1	0.5	0.1	1	1.3684
1	1	0.5	0.1	1	1.4984
1	3	0.5	0.1	1	0.3618
1	5	0.5	0.1	1	0.2036
1	7	0.5	0.1	1	0.1461
1	9	0.5	0.1	1	0.1151
1	1	1	0.1	1	0.9950
1	1	2	0.1	1	0.7433
1	1	3	0.1	1	0.6594
1	1	4	0.1	1	0.6175

ISSN: 2350-0328

International Journal of Advanced Research in Science, Engineering and Technology

Vol. 3, Issue 9 , September 2016

1	1	5	0.1	1	0.5923
1	1	0.5	0.1	1	1.4984
1	1	0.5	0.2	1	1.6308
1	1	0.5	0.3	1	1.7356
1	1	0.5	0.4	1	1.8169
1	1	0.5	0.5	1	1.8789
1	1	0.5	0.1	0.5	0.1930
1	1	0.5	0.1	0.6	0.5185
1	1	0.5	0.1	0.7	0.8232
1	1	0.5	0.1	0.8	1.0910
1	1	0.5	0.1	0.9	1.3159

Table-2 Variation of Shear Stress with ε at the Interface of Lower Permeable Bed (LPB) and Upper Permeable Bed (UPB) (σ =1, P=-1, α =0.5,R=1, λ_1=0.1)

$\tilde{\tau}$	ε =2	ε =3	ε =4	ε =5	ε =6
$nt=\pi/4$					
LPB(at y=-1)	1.2650	1.3672	1.4225	1.4563	1.4788
UPB(at y=1)	-1.2650	-1.3672	-1.4225	-1.4563	-1.4788
$nt=\pi/2$					
LPB(at y=-1)	2.1135	2.3810	2.5433	2.6446	2.7114
UPB(at y=1)	-2.1135	-2.3810	-2.5433	-2.6446	-2.7114
$nt=3\pi/4$					
LPB(at y=-1)	3.0273	3.3924	3.6206	3.7592	3.8454
UPB(at y=1)	-3.0273	-3.3924	-3.6206	-3.7592	-3.8454
$nt=\pi$					
LPB(at y=-1)	3.1222	3.4672	3.6639	3.7648	3.8111
UPB(at y=1)	-3.1222	-3.4672	-3.6639	-3.7648	-3.8111

Table – 3 Variation of Shear Stress with R at the Interface of Lower Permeable Bed (LPB) and Upper Permeable Bed (UPB) (σ =1, P=-1, α =0.5, ε =1, λ_1=0.1)

$\tilde{\tau}$	R=1	R=2	R=3	R=4	R=5
$nt=\frac{\pi}{4}$					
LPB(at y=-1)	1.0637	-0.1473	-1.0581	-1.4843	-1.6349
UPB(at y=1)	-1.0637	0.1473	1.0581	1.4843	1.6349
$nt=\frac{\pi}{2}$					
LPB(at y=-1)	1.7473	0.5181	0.0450	-0.0703	-0.0794
UPB(at y=1)	-1.7473	-0.5181	-0.0450	0.0703	0.0794
$nt=\frac{3\pi}{4}$					
LPB(at y=-1)	2.5425	1.7264	1.4539	1.3931	1.3902
UPB(at y=1)	-2.5425	-1.7264	-1.4539	-1.3931	-1.3902
$nt=\pi$					
LPB(at y=-1)	2.6172	2.2018	2.0311	1.9910	1.9887
UPB(at y=1)	-2.6172	-2.2018	-2.0311	-1.9910	-1.9887

ISSN: 2350-0328

International Journal of Advanced Research in Science, Engineering and Technology

Vol. 3, Issue 9 , September 2016

Table –4 Variation of Shear Stress with σ at the Interface of Lower Permeable Bed(LPB)and Upper Permeable Bed (UPB) (R=1,P=-1, α =0.5, ε =1, λ_1=0.1)

$\tilde{\tau}$	σ =1	σ =3	σ =5	σ =7	σ =9
$nt=\frac{\pi}{4}$					
LPB(at y=-1)	1.0637	0.9832	0.9135	0.8857	0.8712
UPB(at y=1)	-1.0637	-0.9832	-0.9135	-0.8857	-0.8712
$nt=\frac{\pi}{2}$					
LPB(at y=-1)	1.7473	0.9550	0.7041	0.6048	0.5526
UPB(at y=1)	-1.7473	-0.9550	-0.7041	-0.6048	-0.5526
$nt=\frac{3\pi}{4}$					
LPB(at y=-1)	2.5425	0.8581	0.4268	0.2583	0.1699
UPB(at y=1)	-2.5425	-0.8581	-0.4268	-0.2583	-0.1699
$nt=\pi$					
LPB(at y=-1)	2.6172	0.5808	0.1112	-0.0668	-0.1601
UPB(at y=1)	-2.6172	-0.5808	-0.1112	0.0668	0.1601

Table – 5 Variation of Shear Stress with λ_1 at the Interface of Lower Permeable Bed (LPB) and Upper Permeable Bed (UPB) (R=1, P=-1, α =0.5, ε =1, σ =1)

$\tilde{\tau}$	$\lambda_1=0.1$	$\lambda_1=0.2$	$\lambda_1=0.3$	$\lambda_1=0.4$	$\lambda_1=0.5$
$nt=\frac{\pi}{4}$					
LPB(at y=-1)	1.0637	0.9724	0.8721	0.7650	0.6530
UPB(at y=1)	-1.0637	-0.9724	-0.8721	-0.7650	-0.6530
$nt=\frac{\pi}{2}$					
LPB(at y=-1)	1.7473	1.6250	1.4956	1.3642	1.2347
UPB(at y=1)	-1.7473	-1.6250	-1.4956	-1.3642	-1.2347
$nt=\frac{3\pi}{4}$					
LPB(at y=-1)	2.5425	2.4590	2.3686	2.2769	2.1876
UPB(at y=1)	-2.5425	-2.4590	-2.3686	-2.2769	-2.1876
$nt=\pi$					
LPB(at y=-1)	2.6172	2.5907	2.5528	2.5092	2.4636
UPB(at y=1)	-2.6172	-2.5907	-2.5528	-2.5092	-2.4636

ISSN: 2350-0328

International Journal of Advanced Research in Science, Engineering and Technology

Vol. 3, Issue 9 , September 2016

Table – 6 Variation of Shear Stress with α at the Interface of Lower Permeable Bed (LPB) and Upper Permeable Bed (UPB) (R=1, P=-1, λ_1=0.1, ε =1, σ =1)

$\tilde{\tau}$	α =1	α =2	α =3	α =4	α =5
$nt=\frac{\pi}{4}$					
LPB(at y=-1)	0.8828	0.7924	0.7622	0.7472	0.7381
UPB(at y=1)	-0.8828	-0.7924	-0.7622	-0.7472	-0.7381
$nt=\frac{\pi}{2}$					
LPB(at y=-1)	1.0813	0.7483	0.6373	0.5818	0.5485
UPB(at y=1)	-1.0813	-0.7483	-0.6373	-0.5818	-0.5485
$nt=\frac{3\pi}{4}$					
LPB(at y=-1)	1.3817	0.8013	0.6079	0.5111	0.4531
UPB(at y=1)	-1.3817	-0.8013	-0.6079	-0.5111	-0.4531
$nt=\pi$					
LPB(at y=-1)	1.3441	0.7076	0.4954	0.3894	0.3257
UPB(at y=1)	-1.3441	-0.7076	-0.4954	-0.3894	-0.3257

VII. NOMENCLATURE

x, y	Cartesian co-ordinates
$-h$	Width of the channel at lower permeable bed
h	Width of the channel at upper permeable bed
k_1	Permeability of the lower bed
k_2	Permeability of the upper bed
σ_1	$(=h/\sqrt{k_1})$ dimensionless parameter
σ_2	$(=h/\sqrt{k_2})$ dimensionless parameter
u_{B_1}	Slip velocity at the lower bed
u_{B_2}	Slip velocity at the upper bed
Q_1	$-(k_1/\mu)(\partial p/\partial x)$, Darcy's velocity in the lower bed
Q_2	$-(k_2/\mu)(\partial p/\partial x)$, Darcy's velocity in the upper bed
Q	Mass flux
P	Pressure
ρ	Density
n	Frequency
μ	Coefficient of viscosity
α	Slip parameter
τ	Shear stress

ISSN: 2350-0328

International Journal of Advanced Research in Science, Engineering and Technology

Vol. 3, Issue 9 , September 2016

υ	Kinematic viscosity
Re	$(=Uh/\upsilon)$Reynolds number
σ	Porosity parameter
ε	Permeability parameter
λ_1	Jeffrey parameter
U	Average velocity

ACKNOWLEDGMENT

One of the authors Prof. S. Sreenadh express thanks to UGC for providing financial support through the Major Research Project No: F. No. 41-778/2012(SR) to undertake this work.

REFERENCES

[1] Y. C. Wang, Pulsatile flow in a porous channel, Transaction of ASME, J. Appl. Mech. 38 (1971) 553-555.
[2] K. Vajravelu, K. Ramesh, S. Sreenadh, P.V. Arunachalam, Pulsatile flow between permeable beds, Int. J. Non-Linear Mech. Vol.38, 2003, pp. 999-1005
[3] Sankar, D.S., and Hemalatha, K. (2006), Pulsatile flow of Herschel-Bulkley fluid through catheterized arteries – a mathematical model, Applied Mathematical Modeling, Vol.31, No.8, 1497-1517 .
[4] Prashanta Kumar Mandal, SantabrataChakravarty, ArabindaMandal, and Norsarahaida Amin (2007), Effect of body acceleration on unsteady pulsatile flow of non - Newtonian fluid through a stenosed artery, Applied Mathematics and Computation, Vol.189, No.1, 766-779 .
[5] Krishna kumari P., S.V.H.N., Ramana Murthy, M.V., Ravi Kumar, Y.V., and Sreenadh S. (2011), Peristaltic pumping of a Jeffrey fluid under the effect of magnetic field in an inclined channel, Applied Mathematical Sciences, vol.5, No.9, 447-458
[6] Krishna kumari P., S.V.H.N., Ramana Murthy, M.V., Ravi Kumar, Y.V., and Sreenadh, S. (2011), Peristaltic pumping of a Jeffrey fluid in a porous tube, ARPN Journal of Engineering and Applied sciences, vol.6, No.3.
[7] Akbar, N.S., Nadeem, S., and Ali Mohamed (2011), Jeffrey fluid model for blood flow through a tapered artery with a stenosis, Journal of Mechanics in Medicine and Biology(JMMB), vol.11, No.3, 529-545.
[8] Srinivas, S., and Muthuraj, R. (2010), Peristaltic transport of a Jeffrey fluid under the effect of slip in an inclined asymmetric channel, International Journal of Applied Mechanics(IJAM), vol.2, No.2, 437-455.
[9] K.Vajravelu, K. Ramesh, S. Sreenadh and P.V. Arunachalam, Pulstaile flow between permeable beds, international Journal of Non-Linear mechanics, 38 (2003) 999-1005.
[10] E. Sudhakara, S.Sreenadh and G. Bhaskar Reddy, pulsatile flow of a hydromagnetic jeffrey fluid between permeable beds, International Journal of Mathematical Archive-Vol. 3(11), 2012, 4017-4027.
[11] Hemadri Reddy, R., Kavitha, A., Sreenadh, S., and Hariprabakaran, P. (2011), Effect of thickness of the porous material on the peristaltic pumping when the tube wall is provided with non erodible porous lining, Pelagia Research Library, Advances in Applied Science Research, VoL.2., No.2, 167-178.
[12] Vasudev, C., Rajeswar Rao, U., Subba Reddy, M.V., and Prabhakar Rao, G. (2010), Peristaltic pumping of Williamson fluid through a porous medium in a horizontal channel with heat transfer, American Journal of Scientific and Industrial Research,vol.1, No.3, 656-666.
[13] Kim, Albert S., and Yong Taek Lee (2011), Laminar flow with injection through a long dead-end cylindrical porous tube: Application to a hollow fiber membrane, AICHE Journal, Vol.57, No.8, 1997-2006
[14] Srinivas, S., and Kothandapani, M. (2009), The influence of heat and mass transfer onMHD peristaltic flow through a porous space with compliant walls, Applied Mathematics and Computation, Vol.213, No.1,197-208
[15] Vajravelu, K., Radhakrishnamacharya, G., and Radhakrishnamurthy, V. (2007), Peristaltic flow and heat transfer in a vertical porous annulus, with long wave approximation, International Journal of Non-Linear Mechanics, Vol.42, No.5, 754-759
[16] K. LalithaJyothi, P. Devaki and S.Sreenadh, Pulsatile flow of a jeffrey fluid in a circular tube having internal porous lining, International Journal of Mathematical Archive, Vol. 4(5), 2013, 75-82.
[17] K. Vajravelu, P. V. Arunachalam and S. Sreenadh, Unsteady flow of two immiscible conducting fluids between two permeable beds, Journal of Mathematical Analysis and Applications , Vol. 196, 1995, 1105-1116.
[18] Rajasekhara, B.M.,Rudraiah,N. and Ramaiah,.B.K Couette flow over a naturally Permeable bed. Journal of Mathematical and Physical Sciences, vol. 9, pp.49-56, 1975.